

ISSN 2063-5346



SPATIO-TEMPORAL VARIATION IN THE AIRBORNE CHEMICAL POLLUTANTS NEAR OPEN AND COVERED DRAINS OF SOUTH WEST DELHI, INDIA

Asha Jamloki^{1,2}, Ashu Gupta³, Sarita Tehlan⁴, Anuj Ranjan^{5*}, Abhishek Chauhan^{6*}, Reetu Singh⁷, S.K. Tyagi⁸ and Tanu Jindal⁶

Article History: Received: 01.02.2023

Revised: 07.03.2023

Accepted: 10.04.2023

Abstract

In the past few decades, air pollution has become a major environmental problem consistently challenging ecosystems and human health. Air pollution is mostly caused by emission sources such as vehicles, industries, open burning, volcanic eruptions, and others. However, the drains that carry industrial and sewage wastewater in urban settlements are also sources of air pollutants. In the case of Delhi, India, the drains are lined (concreted), unlined, covered, and also open at various locations. In this study, we assessed the air pollution load caused by the drains. The study was conducted around the tributary drains of the Najafgarh-Palam drain in the southwest part of New Delhi. We compared the concentration of chemical air pollutants by monitoring during the morning, evening, and midnight hours from June 2020 to April 2021. We used the Modified Jacobs and Hochheiser method for sampling and analysis of nitrogen dioxide (NO₂) and the Indophenol method for ammonia (NH₃). We sampled and analyzed sulphur dioxide (SO₂) and ozone (O₃) using the West & Geake method and the iodometric method, respectively. The results showed that there is a variation in the concentration of these pollutants in the areas with open and covered drains and at different times of the day in twenty-four hours due to differences in local environmental conditions, vehicular load, human settlement, and activities. This study revealed that leaving the drains open and planting trees on their embankments help to minimize the overall pollution load.

Keywords: Air Pollution, Drains, Sulphur dioxide, Nitrogen dioxide, Ozone, Ammonia

¹Amity Institute of Environmental Sciences, Amity University, Sector-125, Noida-201301, Uttar Pradesh, India

²Environmental Laboratory, Eco-Care Instruments Pvt. Ltd., Dwarka, New Delhi, India

³Department of Chemistry, Shyamlal College (University of Delhi), Shahdara, New Delhi-110032, India

⁴Department of Chemistry, Motilal Nehru College (University of Delhi), Benito Juarez Marg, New Delhi -110021, India

⁵Academy of Biology and Biotechnology, Southern Federal University, Rostov-on-Don, Russia, 344006

⁶Amity Institute of Environmental Toxicology, Safety and Management, Amity University, Sector-125, Noida-201301, Uttar Pradesh, India

⁷Department of Chemistry, S.S.V. (P.G.) College, Hapur-245101, Uttar Pradesh, India

⁸Central Pollution Control Board, Government of India, New Delhi, India

Corresponding authors: aranjan@amity.edu; akchauhan@amity.edu

DOI: 10.31838/ecb/2023.12.4.057

INTRODUCTION:

Clean air is one of the basic requirements of human existence. Air pollution has degraded the environment for humans and other organisms and continues to pose significant threats to human and environmental health worldwide [1]. Whereas the gases, particulates and microbes can cause diseases and cause damage to materials, the odour-generating gases make stench annoying. Air pollutants harm human health and cause diseases of heart, stroke and respiratory cancers, neurological impairments, and increased risk of fetal mortality and morbidity [2]. Sulphur dioxide (SO₂), Nitrogen oxides (NO_x), Ozone (O₃), Carbon monoxide (CO) and odorous gases like Ammonia (NH₃), Hydrogen Sulphide (H₂S) are the major contributors to air pollution [3]. According to WHO particulate air pollution causes an estimated 7 million deaths annually, or one in eight premature deaths every year [4]. The majority of these deaths happen in the Asian and African continent which has the most under-developed and developing nations. This makes it the world's largest environmental public health risk and among the largest global health risks comparable with "traditional" health risks such as smoking, high cholesterol, high blood sugar and obesity WHO World Air Quality report, 2020.

Among the air pollutants ozone is one of the harmful pollutants for humans as well as the ecosystem if it is in the lower layer of the troposphere [5]. Its formation takes place when precursor chemicals like carbon monoxide, methane, volatile organic compounds (VOC's) and nitrogen oxides (NO_x) produced by combustion of fuel and evaporation from vehicles, power plant, refineries, gasoline dispensing, print shop, paints, *etc.* [6] react in the presence of sunlight. A study has shown that there may be extra 40-60 deaths per 100,000 persons in India due to ozone induces respiratory diseases [7]. Short-term exposure to ambient ozone was linked to greater non-accidental and cardiovascular mortality, according to a study conducted in China [8]. Additionally, it was projected in year 2016 that long-term O₃ exposure was responsible for 23.0-40.3 million respiratory-related deaths [7]. It could become a greater threat in India if major mitigation measures focus on particulate matter (P.M.) pollution alone [9].

Environmental pollutants like PM_{2.5}, O₃ and CO are positively correlated with an increase in SARS-CoV-2 cases and deaths each day in London, U.K. [10].

Emissions from transport and industrial sectors are responsible for toxic pollutants such as NO_x and SO_x in air and hence accurate and periodic monitoring is grave requirement at the current scenarios [11]. SO₂ and NO₂ have serious environmental and health consequences [12]. They are largely contributed by combustion of fuels in vehicles, thermal power plants and industries [13]. NO₂ is precursor of ground level O₃, acid rain and P.M. pollutants [14]. Chronic exposure to NO₂ has been reported to cause respiratory dysfunction and reduced lung capacity [15]. SO_x causes respiratory tract irritation and increases the risk of infection. It causes excessive coughing, mucus formation, and aggravates the asthma and chronic bronchitis [16].

Together with sulphur dioxide (SO₂) and nitrogen oxides, atmospheric NH₃ influences the deposition of acidic compounds in the environment. It is the reduced form of nitrogen (NO_x). On deposition, it contributes significantly to the biogeochemical processes in delicate ecosystems such forests, rivers, coastal areas, and soil. NH₃ can react with atmospheric acids (H₂SO₄, HNO₃, or HCl) to produce secondary airborne particles like (NH₄)₂SO₄, NH₄NO₃, and NH₄Cl, among others [17]. NH₃ helps to create N₂O, a potent greenhouse gas that exacerbates the issue in most cases but also helps to chill the planet by promoting the creation of particulate matter and clouds [18]. NH₃ is a colourless pungent gaseous pollutant (detection threshold of 1.5 ppm) is contributed by agriculture practices, including animal husbandry and the use of NH₃-based fertilizers [19]. However, industrial processes, vehicular emissions, and volatilization from soils and oceans are also sources of NH₃ [20]. At level 20-50 ppm it can cause sensory irritation in eyes and lungs airways [21]. Extremely high levels of NH₃ can cause lung damage or death [22].

According WHO, death due to ambient (outdoor) air pollution was estimated to cause 4.2 million premature deaths worldwide due to exposure to fine particulate matter, which causes cardiovascular and

respiratory disease, as well as cancers. Most air pollution-related deaths are from heart disease and stroke, followed by chronic obstructive pulmonary disease, acute and chronic respiratory conditions and cancers [23]. The Indian National Ambient Air Quality Standards [24] has recommended the time weighted average (TWA) of 24 hrs of exposure of SO₂, NO₂, and NH₃ as 80 µg/m³, 80 µg/m³, 400 µg/m³ respectively and TWA of 8 hours of exposure of O₃ as 100 µg/m³. The WHO Air Quality Guidelines [25] states that the maximum permissible TWA exposure of PM_{2.5}, PM₁₀, O₃, NO₂, SO₂, CO for 24 hr are 15 µg/m³, 45 µg/m³, 25 µg/m³, 40 µg/m³, 4 mg/m³ respectively and TWA of 8 hours of exposure of O₃ as 100 µg/m³.

The sources of air pollution are usually thermal power plants, transportation, industrial activities, construction, burning of crop wastes etc. However, the drains that carry sewage and industrial wastes have also been reported to contribute air pollutants [26]. Therefore, in this research we aimed to study and monitor the chemical air pollution faced by the general population that are habituated in vicinity of the drains. The major target of this study is to assess the concentration trends of SO₂, NO₂, NH₃, and O₃ across the seasons, distance from drains, and how the closing the drains and leaving them open is useful in masking the emission of these gaseous pollutants to prevent air pollution.

2. MATERIALS AND METHODS

2.1 Chemicals and reagents:

The chemicals used for analyzing the samples were of analytical reagent grade sourced from Merck and Fischer Scientific. The chemicals and reagents used were as under:

Sulphur dioxide: Mercuric chloride, sodium chloride, EDTA di-sodium salt, absorbing reagent: 0.04 M potassium tetrachloromercurate (TCM), sulphamic acid (0.6%), formaldehyde (0.2%), purified pararosaniline stock solution (0.2% nominal), pararosaniline working solution, stock iodine solution (0.1 N), iodine solution (0.01 N) starch indicator, potassium iodate, stock sodium thiosulfate solution (0.1 N), sodium thiosulphate titrant (0.01 N), sodium

metabisulphite (Na₂S₂O₅) for preparing standard and working sulphite-TCM solution

Nitrogen dioxide: Sodium hydroxide, sodium arsenite for making absorbing solution, sulphanilamide, N-(1-Naphthyl)-ethylenediamine Di-hydrochloride (NEDA), hydrogen peroxide - 30%, phosphoric acid - 85%, sodium nitrite - assay of 97% NaNO₂ for preparation of standards

Ozone: Absorbing solution (1% KI in 0.1 M phosphate buffer), stock solution 0.025 M I₂ (0.05 N)

Ammonia: 1N Sulphuric acid (absorbing solution), sodium nitroprusside, 6.75 M sodium hydroxide, sodium hypochlorite solution, phenol solution 45% v/v, sodium phosphate, ammonium chloride or ammonium sulfate, hydrochloric acid, ammonium chloride for ammonia stock solution (1 mg NH₃/mL)

2.2 Major equipment

The monitoring and analysis of chemical pollutants in ambient air were done using Shimadzu Analytical balance (0.1 mg), Vacuum pumps, calibrated flow-meters to control the airflow from 0.2 to 2 l/min, glass midjet impingers, UV-visible spectrophotometer and A grade volumetric glassware.

All the equipment was calibrated by NABL-accredited laboratories to maintain traceability to international SI units. Intermediate checks were done on equipment and standards that were also calibrated by NABL-accredited laboratories.

2.3 Methodology

2.3.1 Sampling

30 mL of pollutant-specific absorbing media was poured into the bubblers and connected to the gas sampling attachments of the low volume samplers of make Dutt Instrumentation. The samplers were installed in such a manner that the air inlet was at a height of more than 3 meters above ground and was located 10 meters from the main source of a pollutant which is the drain or heavy traffic flow and road. Air was drawn at

the rate of 1 LPM for 4 hours. After sampling the volume of the absorbing solution was checked in the bubblers and any loss due to evaporation was made up by adding distilled water. The exposed absorbing solutions were then transferred to the storage bottles and preserved. They were then taken to the laboratory for analysis or stored in the refrigerator for further use. For each pollutant field blank was also exposed to environmental conditions except that air was not bubbled into them.

2.3.2 Analysis of sulphur dioxide

West & Gaeke method (IS 5182 part 2) for sampling and analysis of SO₂ in ambient air which works for the concentration range of 25 to 1050 µg/m³ was followed. SO₂ present in the air was absorbed in a 30 mL solution of potassium tetrachloromercurate (TCM) to form a di-chloro-sulphitomercurate complex. Out of 30 mL of exposed absorbing solution 25 mL was taken in the 25 mL volumetric flask. To it, 1 mL sulphamic acid was added and left to react for 10 minutes to destroy the NO₂⁻ resulting from oxides of nitrogen. This was followed by the addition of 2 mL formaldehyde and 2 mL working pararosaniline solution and left for 30 minutes to react to form the intensely coloured pararosaniline methyl sulphonic acid. Reagent blank, field blank and calibration standards in the range 4.0 µg to 24.12 µg were also prepared in a 25 mL volumetric flask and treated similarly. The absorbance of each of the flasks was taken on a UV-visible spectrophotometer at 560 nm using distilled water as a reference. The calibration graph was plotted using MS excel and the calibration factor was obtained that was used to calculate the concentration of SO₂ in µg/m³.

Calculation:

$$C(\text{SO}_2) = (A_s - A_b) \times + \frac{CF \times V_s}{V_a \times V_t}$$

where,

C (SO₂) = Concentration of SO₂ in µg/m³

A_s = Absorbance of sample

A_b = Absorbance of the reagent blank

CF = Calibration factor

V_a = Volume of air sampled, m³

V_s = Volume of sample from field, mL

V_t = Volume of aliquot taken for analysis, mL

2.3.3 Analysis of nitrogen dioxide

Modified Jacobs & Hochheiser method (IS 5182 part 6) [27] for sampling and analysis of NO₂ in the air was followed. The nominal range of the method is 6 to 750 NO₂ µg/m³. Ambient NO₂ was collected by bubbling air through a 30 mL solution of sodium hydroxide and sodium arsenite. 10 mL from the 30 mL of the sample obtained from the site was taken into a 50 mL volumetric flask and 1 mL of hydrogen peroxide solution, 10 mL of sulphanilamide solution, and 1.4 mL of N-(1-naphthyl)-ethylenediamine dihydrochloride (NEDA) solution was added and thoroughly mixed after each addition and diluted to 50 mL mark with distilled water and allowed to rest for 10 minutes for NO₂⁻ ions formed during sampling to react with phosphoric acid, sulphanilamide, and NEDA to form pink colour. Similarly, reagent blank, field blank and calibration standards in the range of 1 µg to 25 µg were also prepared. The absorbance of each was noted from the UV-Vis spectrophotometer at 540 nm taking distilled water as a reference. The graph was plotted using MS excel for absorbance versus concentration and a calibration factor was obtained to calculate the amount of NO₂.

Calculation

$$C(\text{NO}_2) = (A_s - A_b) \times + \frac{CF \times V_s}{V_a \times V_t} \times 0.82$$

where,

C(NO₂) = Concentration of nitrogen dioxide in µg/m³

A_s = Absorbance of sample

A_b = Absorbance of the reagent blank

CF = Calibration factor

V_a = Volume of air sampled, m³

V_s = Volume of the sample obtained from field, mL

V_t = Volume of aliquot taken for analysis, mL

0.82 = Sampling efficiency

2.3.4 Analysis of ozone

The iodometric method (IS 5182 part 9) [28] was used for the manual determination of O₃ in concentrations between 0.01 and 10 ppm as O₃. It works on the principle that micro-amounts of O₃ and the oxidants liberate iodine when absorbed in a 1% solution of potassium iodine buffered at pH 6.8 ± 0.2. The iodine is determined spectrophotometrically by measuring the absorption of the tri-iodide ion at 352 nm. So, within 60 min after the sample collection, the absorbance of the 10 mL sample was observed against a reference cuvette containing distilled water. The absorbance of the unexposed reagent was subtracted from the absorbance of the sample. A calibration graph in the range of 1.962 µg to 9.81 µg was prepared using a standard iodine solution to obtain the calibration factor.

Calculation

$$C(O_3) = (A_s - A_b) \times CF \times \frac{1.92}{(V_a)}$$

where,

C(O₃) = Concentration of O₃ in µg/ m³

A_s = Absorbance of sample

A_b = Absorbance of the reagent blank

CF = Calibration factor

V_a = Volume of air sampled in m³

1.962 = Conversion factor, µl to µg

2.3.5 Analysis of ammonia

The Indophenol method (IS 5182 Part 25) [29] was followed for testing and sampling of NH₃ in the air with a sampling rate of 1 l/min for 1 hour. It works for a concentration range of 20 to 700 µg/m³. This method works on the principle that atmospheric NH₃ forms (NH₄)₂SO₄ when bubbled into a dilute solution of H₂SO₄. The (NH₄)₂SO₄ can then be analyzed using a spectrophotometer by reaction with phenol and alkaline sodium hypochlorite to produce indophenol. So a 10

sample, field blank, reagent blank and calibration standards in the range 1 µg to 20 µg was transferred to a 25 mL volumetric flask at 25°C and 2 mL buffer was added followed by 5 mL of working phenol solution and mixed and filled to about 22 mL. Then 2.5 mL of working hypochlorite solution was added and rapidly mixed. The solutions were then diluted to 25 mL, mixed and stored in the dark for 30 minutes to develop the blue colour of indophenol. The absorbance of the solutions was measured at 630 nm on a UV-Vis spectrophotometer using 1 cm cells. The graph was plotted using MS excel and a calibration factor was obtained to calculate the concentration of ammonia in µg/ m³.

Calculation

$$C(NH_3) = (A_s - A_b) \times \frac{CF}{(V_a)}$$

where,

C(NH₃) = Concentration of ammonia in µg/m³

A_s = Absorbance of sample

A_b = Absorbance of the reagent blank

CF = Calibration factor

V_a = Volume of air sampled in m³

3. Study area

The study area for this project was two locations on the sister drains of the main Najafgarh drain-the Palam drain in New Delhi, India. The Palam Drain is 8.78 Km long. It originates from Delhi Cantonment and passes through residential areas of Sagarpur, Raghu Nagar, Dabri, Sitapuri, Vijay Nagar, Mahavir Enclave, Madhu Vihar, Dwarka to terminate into the Najafgarh Drain. A stretch of 2.3 km of this drain is covered by the Delhi Development Authority and converted into a road –The Dabri Dwarka Road or the Nala Road. One of the locations of monitoring was a covered drain at Dabri Dwarka Nala Road (L1) and the other was an open drain near CNG Filling Gas Station, Sector-5, Dwarka (L2).

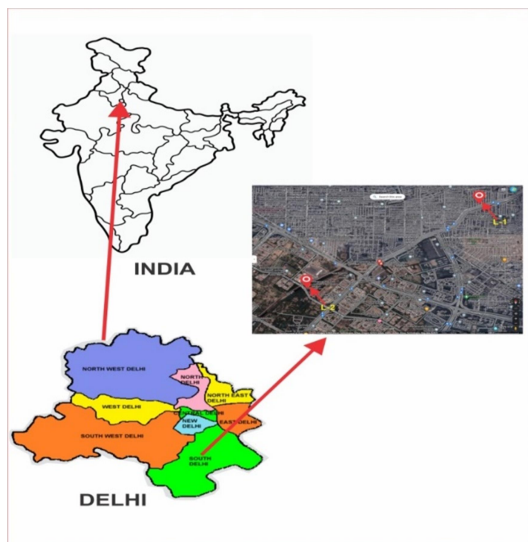


Fig. 1. Study area in Southwest Delhi

3.1 Data collection

The sampling of pollutants was done for 10 days continuously for an interval of 4 hrs in the morning (8:00 A.M. to 12:00 P.M.), evening (4:00 P.M. to 8:00 P.M.) and night (12 A.M. to 4:00 A.M.). These three distinct times were chosen to cover all the possible conditions of traffic and human activities that affect the environmental conditions. Time after midnight does not have traffic, the morning hours from 8 A.M. to 12 noon is an active period and the evening hours from 4 P.M. to 8 P.M. are the peak hours for traffic. Sampling

and subsequent testing were done as per the method described in Section 2.3. The meteorological parameters, temperature, wind speed, relative humidity and solar radiation were taken from the Sector 8, Dwarka, Dew Delhi monitoring site run by the Delhi Pollution Control Board, New Delhi.

4. RESULTS

4.1 Assessment of pollutant concentration Location 1 (L1)

The experimental results showed that the concentration of NO_2 in the morning (8 A.M. to 12 P.M.) was found in the range of $15.63 \pm 3.3 \mu\text{g}/\text{m}^3$ to $50.88 \pm 6.43 \mu\text{g}/\text{m}^3$. It was highest in November 2020 and the lowest in January 2021. The level of NH_3 pollution observed was found to be maximum in March 2021 with a concentration of $70.99 \pm 10.29 \mu\text{g}/\text{m}^3$ and least in July 2020 at $13.72 \pm 1.79 \mu\text{g}/\text{m}^3$. However, SO_2 was found in increased concentration in April 2021 at $21.64 \pm 7.44 \mu\text{g}/\text{m}^3$ and in July 2020 it was the lowest at $2.83 \pm 1.03 \mu\text{g}/\text{m}^3$ concentration. The concentration of O_3 was found in the range of $15.14 \pm 3.95 \mu\text{g}/\text{m}^3$ in January 2021 to $76.03 \pm 10.58 \mu\text{g}/\text{m}^3$ in June 2020. Table-1 represents the concentration of NO_2 , NH_3 , SO_2 , and O_3 at location 1 from June 2020 to April 2021 and Fig. 2 represents the variation in pollutant concentration at location 1 from June 2020 to April 2021 during 8 A.M. to 12 P.M.

Table-1: Pollution load observed during the morning (8 A.M. – 12 P.M.) monitoring at Location 1

Month	Mean concentration of pollutants (in $\mu\text{g}/\text{m}^3$) with standard deviation			
	NO_2	NH_3	SO_2	O_3
Jun-20	29.31 ± 5.33	15.97 ± 1.23	3.33 ± 0.75	76.03 ± 10.58
Jul-20	28.89 ± 4.37	13.72 ± 1.79	2.83 ± 1.03	44.67 ± 6.87
Aug-20	37.64 ± 7.34	17.23 ± 3.66	6.10 ± 0.66	33.56 ± 5.84
Sep-20	33.79 ± 8.56	29.13 ± 5.25	3.45 ± 0.78	22.14 ± 3.41
Oct-20	30.86 ± 2.76	23.25 ± 2.42	16.70 ± 5.13	29.32 ± 5.36
Nov-20	50.88 ± 6.43	38.21 ± 8.64	12.25 ± 3.44	27.20 ± 3.79
Dec-20	22.05 ± 8.4	33.50 ± 4.56	8.55 ± 5.31	17.67 ± 5.91
Jan-21	15.63 ± 3.3	29.55 ± 4.44	6.26 ± 1.75	15.14 ± 3.95
Feb-21	32.30 ± 3.82	46.14 ± 9.74	12.50 ± 3.15	17.83 ± 3.87
Mar-21	31.5 ± 6.34	70.99 ± 10.29	13.81 ± 2.55	29.97 ± 6.08
Apr-21	26.40 ± 6.38	42.42 ± 7.98	21.64 ± 7.44	32.17 ± 5.95

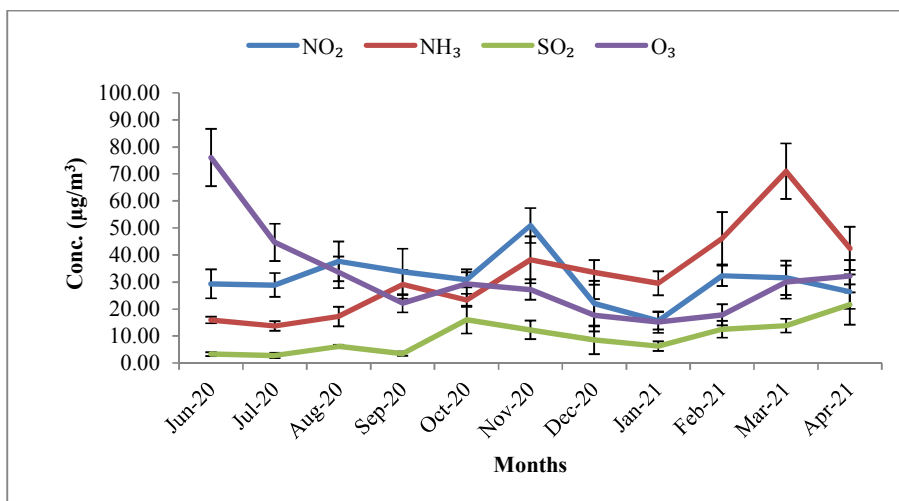


Fig. 2. Comparative analysis of pollutants at Location 1 during the morning (8 A.M. – 12 P.M.)

The present study showed that the concentration of NO₂ in the evening (4 P.M. to 8 P.M.) was in the range of 18.75 ± 5.19 µg/m³ to 65.35 ± 9.32 µg/m³. It was highest in November 2020. However, the concentration was observed lowest in January 2021. The level of NH₃ pollution observed was recorded as highest in February 2021 with a concentration of 89.02 ± 11.18 µg/m³ and least in July 2020 at 15.48 ± 2.18 µg/m³. However, SO₂ was in elevated concentration in March 2021 at 31.32 ± 5.42 µg/m³ and in June 2020 it

was the lowest at 4.71 ± 0.90 µg/m³ concentration. The O₃ was in the range of 17.61 ± 4.39 µg/m³ (January 2021) to 72.69 ± 14.72 µg/m³ (June 2020). Table-2 is representing the concentration of NO₂, NH₃, SO₂, and O₃ at location 1 from June 2020 to April 2021 in the evening time (4 P.M. – 8 P.M.). Fig. 3 represents the variation in pollutant concentration at location 1 from June 2020 to April 2021 in the evening (4 P.M. – 8 P.M.).

Table-2: Pollution load observed during the evening (4 P.M. – 8 P.M.) monitoring at Location 1

Month	Mean concentration of pollutants (in µg/m ³) with standard deviation			
	NO ₂	NH ₃	SO ₂	O ₃
Jun-20	31.81 ± 3.55	17.03 ± 3.11	4.71 ± 0.90	72.69 ± 14.72
Jul-20	30.77 ± 4.30	15.48 ± 2.18	5.06 ± 0.25	53.17 ± 13.94
Aug-20	41.21 ± 8.07	18.89 ± 5.17	6.72 ± 0.62	52.29 ± 8.78
Sep-20	37.00 ± 4.86	30.71 ± 8.77	6.38 ± 1.08	32.55 ± 8.08
Oct-20	43.58 ± 6.52	25.90 ± 4.70	20.49 ± 4.46	36.90 ± 9.40
Nov-20	65.35 ± 9.32	44.44 ± 8.32	23.90 ± 5.35	29.01 ± 8.69
Dec-20	29.65 ± 8.07	38.37 ± 5.11	20.21 ± 2.48	20.96 ± 2.34
Jan-21	18.75 ± 5.19	34.07 ± 4.46	11.39 ± 2.84	17.61 ± 4.39
Feb-21	38.02 ± 4.87	89.02 ± 11.18	21.09 ± 4.85	29.70 ± 4.87
Mar-21	41.92 ± 8.73	85.97 ± 12.10	31.32 ± 5.42	33.89 ± 4.44
Apr-21	33.34 ± 5.62	57.53 ± 12.44	30.58 ± 2.34	37.31 ± 4.50

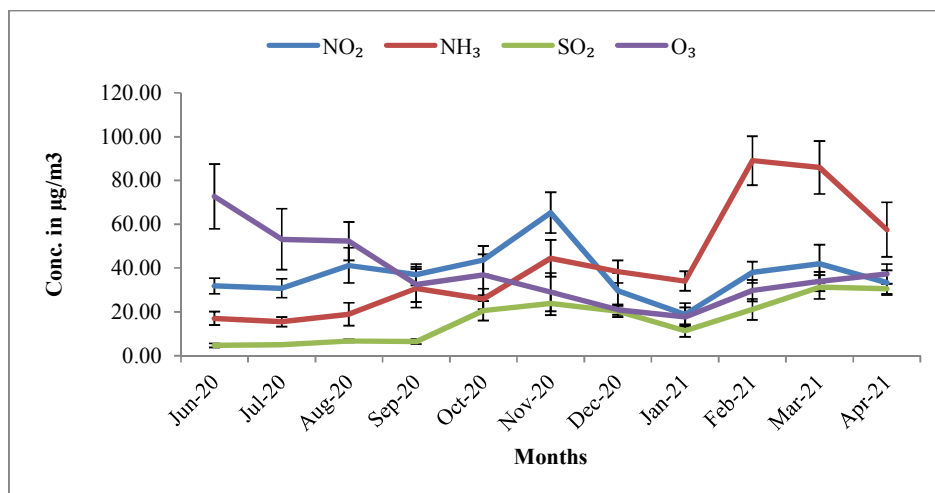


Fig. 3. Comparative analysis of pollutants at location 1 during evening (4 P.M. - 8 P.M.)

The concentration of NO₂ at the night (12 A.M. to 4 A.M.) was in the range of 15.54 ± 2.21 µg/m³ (January 2021) to 38.23 ± 8.74 µg/m³ (March 2021). NH₃ pollution observed was found highest in March 2021 at a level of 78.40 ± 10.38 µg/m³ and least in July 2020 at 9.36 ± 3.93 µg/m³. The SO₂ levels were found elevated in April 2021 at a concentration of

29.24 ± 8.58 µg/m³ and it was the lowest at 2.64 ± 0.42 µg/m³ concentration in July 2020. The O₃ was seen highest in July 2020 (28.98 ± 6.44 µg/m³) and lowest in December 2020 (7.47 ± 4.34 µg/m³) as shown in Table-3. Fig. 4 represents the variation in pollutant concentration at location 1 from June 2020 to April 2021 at the night (12 A.M. – 4 A.M.).

Table-3: Pollution load observed after midnight from 12 A.M. to 4 A.M. monitoring at Location 1

Month	Mean concentration of pollutants (µg/m ³) with standard deviation			
	NO ₂	NH ₃	SO ₂	O ₃
Jun-20	28.20 ± 8.48	15.85 ± 4.01	3.95 ± 0.71	25.25 ± 2.98
Jul-20	20.87 ± 2.52	9.36 ± 3.93	2.64 ± 0.42	28.98 ± 6.44
Aug-20	30.48 ± 4.23	14.51 ± 3.26	6.11 ± 0.53	24.68 ± 3.92
Sep-20	34.18 ± 6.12	25.79 ± 5.79	4.05 ± 1.42	16.53 ± 2.42
Oct-20	33.16 ± 6.51	30.70 ± 4.23	12.28 ± 4.11	21.51 ± 5.31
Nov-20	55.18 ± 9.50	56.81 ± 9.78	15.77 ± 3.83	12.28 ± 4.60
Dec-20	28.41 ± 4.11	48.89 ± 7.91	9.41 ± 3.65	7.47 ± 4.34
Jan-21	15.54 ± 2.21	52.16 ± 7.44	9.14 ± 3.47	9.19 ± 3.05
Feb-21	30.73 ± 4.72	58.94 ± 7.50	13.51 ± 3.64	8.13 ± 3.97
Mar-21	38.23 ± 8.74	78.40 ± 10.38	29.24 ± 8.58	18.65 ± 4.97
Apr-21	17.46 ± 3.02	72.77 ± 13.22	24.84 ± 9.78	13.69 ± 4.77

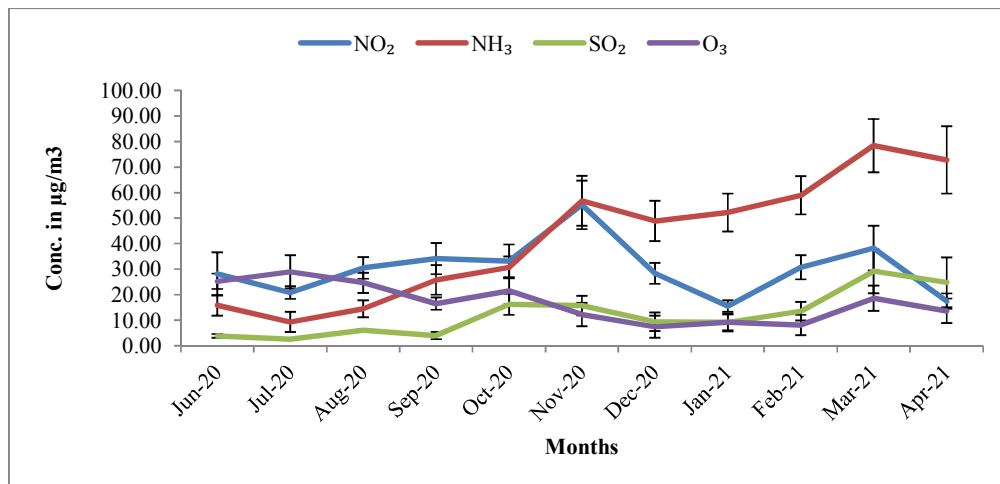


Fig. 4. Comparative analysis of pollutants after midnight 12 A.M. – 4 A.M. at L1

4.2 Assessment of air pollutants at Location 2 (L2)

The concentration of NO₂ in the Morning (8 A.M. to 12 P.M.) was in the range of 12.00 ± 4.02 µg/m³ (August 2020) to 20.43 ± 4.69 µg/m³ (March 2021). NH₃ pollution level observed was highest in February 2021 at a concentration of 35.55 ± 5.84 µg/m³ and lowest in July 2020 at 11.06 ± 1.43 µg/m³. Also, it shall be noted that SO₂ was found at increased levels in October 2020 at 9.54 ± 3.84

µg/m³ and in June 2020 it was the lowest at 1.38 ± 0.44 µg/m³ concentration. The O₃ was highest in June 2020 (30.17 ± 9.02 µg/m³) and lowest in January 2021 (7.82 ± 3.40 µg/m³). Table-4 is representing the concentration of NO₂, NH₃, SO₂, and O₃ at location 2 from June 2020 to April 2021 during the 8 A.M. to 12 P.M. period at L2. Fig. 5 represents the graphical variation in pollutant concentration at location 2 from June 2020 to April 2021 during the 8 A.M. to 12 P.M. period at L2.

Table-4: Pollution load observed during morning (8 A.M. to 12 A.M.) monitoring at Location 2

Month	Mean concentration of pollutants (µg/m ³) with standard deviation			
	NO ₂	NH ₃	SO ₂	O ₃
Jun-20	17.80 ± 2.97	13.16 ± 1.25	1.38 ± 0.44	30.17 ± 9.02
Jul-20	15.43 ± 2.64	11.06 ± 1.43	1.59 ± 0.93	28.76 ± 8.33
Aug-20	12.00 ± 4.02	15.35 ± 3.82	3.23 ± 1.17	24.80 ± 4.55
Sep-20	12.95 ± 3.16	24.74 ± 9	2.54 ± 1.02	17.02 ± 3.53
Oct-20	16.15 ± 2.98	22.55 ± 2.49	9.54 ± 3.84	23.97 ± 7.83
Nov-20	17.48 ± 4.69	33.31 ± 8.11	8.02 ± 2.40	13.48 ± 3.78
Dec-20	12.37 ± 2.32	28.10 ± 4.48	2.83 ± 1.30	8.99 ± 3.06
Jan-21	14.32 ± 2.31	23.57 ± 2.51	5.02 ± 3.43	7.82 ± 3.40
Feb-21	16.60 ± 6.79	35.55 ± 5.84	7.81 ± 3.50	9.47 ± 4.80
Mar-21	20.43 ± 4.69	31.40 ± 3.75	9.06 ± 2.19	17.07 ± 5.52
Apr-21	14.44 ± 2.94	27.01 ± 6.12	9.21 ± 5.02	21.69 ± 5.85

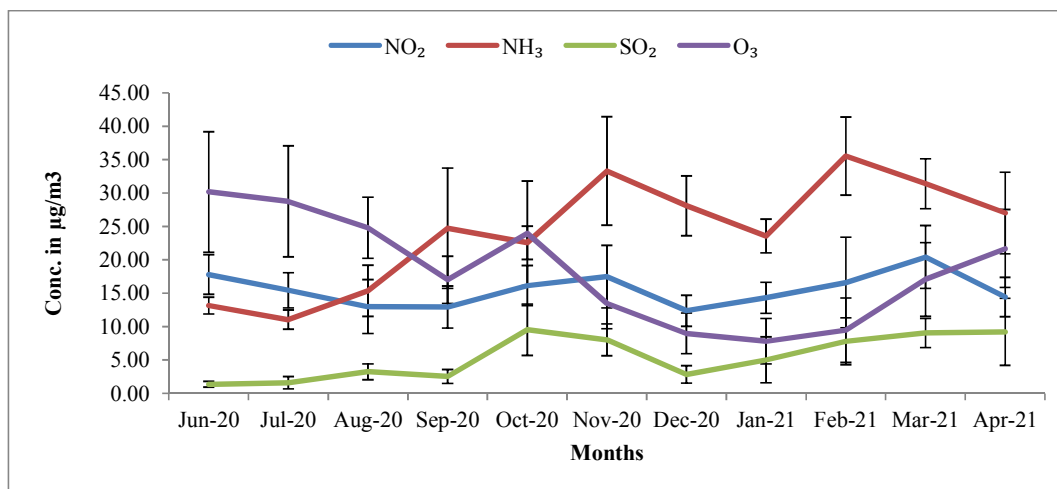


Fig. 5. Comparative analysis of pollutants at location 2 during the morning (8 A.M. - 12 P.M.)

Table-5 shows the observed concentration of NO₂, NH₃, SO₂, and O₃ at location 1 from June 2020 to April 2021 during the evening time (4 P.M. – 8 P.M.). The level of NO₂ in the evening was in the range of 14.54 ± 2.72 µg/m³ (September 2020) to 27.13 ± 4.49 µg/m³ (March 2021). The concentration of NH₃ was recorded as highest in February 2021 at the level of 43.61 ± 7.34 µg/m³ and lowest in July 2020 at 12.95 ± 1.8 µg/m³. SO₂ was in

increased levels in November 2020 at 17.60 ± 3.63 µg/m³ and in June 2020 was the lowest with 2.44 ± 0.75 µg/m³ of concentration. Ozone (O₃) was in the range of 8.78 ± 2.41 µg/m³ to 40.57 ± 10.11 µg/m³ for January 2021 and June 2020 respectively. Fig. 6 represents the graphical variation in pollutant concentration at location 2 from June 2020 to April 2021 in the evening (4 P.M. – 8 P.M.).

Table-5: Pollution load observed during the evening (4 P.M. - 8 P.M.) monitoring at Location 2

Month	Mean concentration of pollutants (in µg/m ³) with standard deviation			
	NO ₂	NH ₃	SO ₂	O ₃
Jun-20	22.66 ± 2.59	16.43 ± 3.13	2.44 ± 0.75	40.57 ± 10.11
Jul-20	17.27 ± 3.90	12.95 ± 1.8	2.46 ± 0.92	30.48 ± 8.87
Aug-20	16.10 ± 5.96	16.69 ± 3.69	5.34 ± 1.24	30.12 ± 5.66
Sep-20	14.54 ± 2.72	27.63 ± 5.35	4.06 ± 0.65	21.05 ± 2.53
Oct-20	17.75 ± 3.59	32.10 ± 4.28	15.21 ± 4.73	12.55 ± 7.73
Nov-20	22.81 ± 3.34	37.49 ± 7.57	17.60 ± 3.63	15.28 ± 3.75
Dec-20	16.53 ± 4.43	32.16 ± 5.07	8.55 ± 2.31	12.51 ± 4.10
Jan-21	24.48 ± 3.10	27.74 ± 3.94	6.56 ± 2.39	8.78 ± 2.41
Feb-21	23.22 ± 8.04	43.61 ± 7.34	8.27 ± 2.95	17.32 ± 5.21
Mar-21	27.13 ± 4.49	39.71 ± 5.02	12.18 ± 4.51	24.81 ± 5.14
Apr-21	26.96 ± 3.58	36.16 ± 7.01	17.27 ± 7.46	25.61 ± 3.95

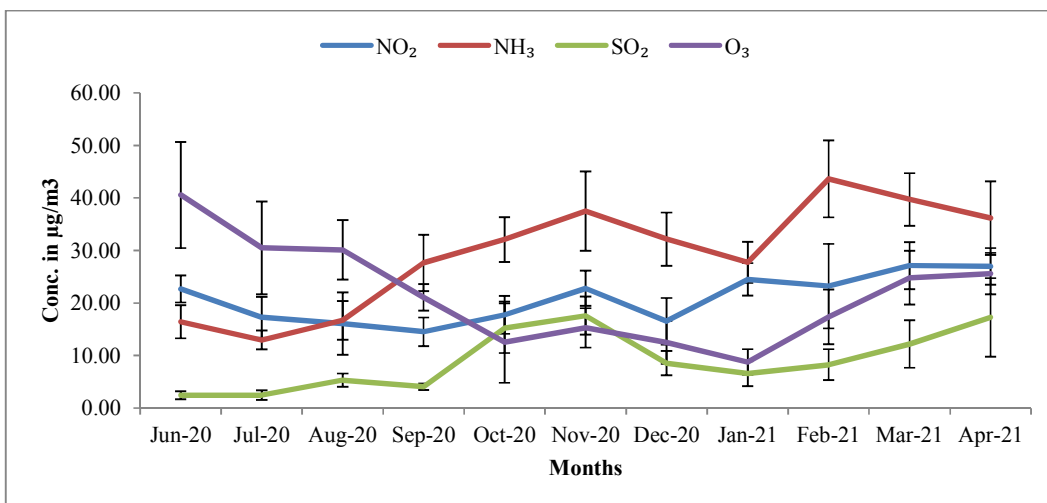


Fig. 6. Comparative analysis of pollutants at location 2 during evening (4 P.M. - 8 P.M.)

The midnight to 4 A.M. observation results showed the concentration of NO₂ in the range of 12.56 ± 3.66 µg/ m³ to 23.13 ± 5.08 µg/ m³. It was lowest in September 2020 and highest in March 2021. The level of NH₃ pollution observed was recorded as highest in November 2020 with a concentration of 56.31 ± 6.78 µg/ m³ and lowest in August 2020 at 13.96 ± 3.27 µg/ m³. However, SO₂ was in the highest concentration in April 2021 at 13.74 ± 6.55 µg/ m³ and in September 2020 it was the

lowest at 2.62 ± 1.13 µg/ m³ concentration. The O₃ concentration was in the range of 2.20 ± 1.06 µg/ m³ (October 2020) to 20.38 ± 5.07 µg/m³ (August 2020). Table-6 is representing the concentration of NO₂, NH₃, SO₂, and O₃ at location 2 from June 2020 to April 2021 from midnight to 4am period and Fig. 7 represents the variation in pollutant concentration at location 2 from June 2020 to April 2021 in the same period.

Table-6: Pollution load observed after midnight from 12 A.M. to 4 A.M. monitoring at Location 2

Month	Mean concentration of pollutants (in µg/m ³) with standard deviation			
	NO ₂	NH ₃	SO ₂	O ₃
Jun-20	16.8 ± 5.60	15.21 ± 4.04	3.40 ± 2.06	15.39 ± 1.73
Jul-20	16.25 ± 4.81	18.59 ± 3.88	2.98 ± 1.20	13.93 ± 4.69
Aug-20	14.52 ± 4.36	13.96 ± 3.27	4.31 ± 0.77	20.38 ± 5.07
Sep-20	12.56 ± 3.66	31.93 ± 4.87	2.62 ± 1.13	15.64 ± 3.47
Oct-20	15.35 ± 4.65	35.00 ± 4.28	11.74 ± 3.96	2.20 ± 1.06
Nov-20	16.72 ± 3.59	56.31 ± 6.78	9.29 ± 1.67	5.30 ± 2.15
Dec-20	14.88 ± 3.24	48.39 ± 7.91	7.51 ± 2.91	6.55 ± 1.14
Jan-21	20.67 ± 4.81	31.55 ± 7.42	6.62 ± 1.80	5.76 ± 1.66
Feb-21	19.71 ± 8.95	56.00 ± 8.19	7.99 ± 4.28	5.50 ± 2.41
Mar-21	23.13 ± 5.08	50.22 ± 10.54	7.46 ± 2.33	10.51 ± 5.69
Apr-21	22.40 ± 6.24	42.51 ± 4.86	13.74 ± 6.55	7.19 ± 3.05

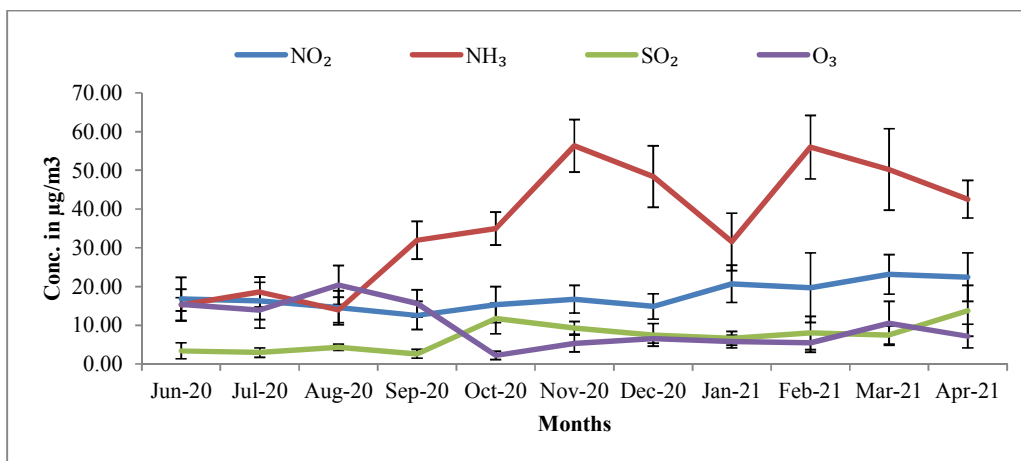


Fig. 7. Comparative analysis of pollutants at location 2 during midnight (12 A.M. – 4 A.M.)

4.2 Meteorological Conditions

The meteorological parameters, Ambient temperature (AT), wind speed (WS), relative humidity (RH) and solar radiation (SR) influence the concentration of air pollutant in a region, hence these data were downloaded for all the three observational time periods (8 A.M. to 12 P.M., 4 P.M. to 8 P.M. and 12 A.M. to 4 A.M.) of the day for 10 days each month from June 2020 to April 2021 from the

Sector 8, Dwarka, Dew Delhi monitoring site run by the Delhi Pollution Control Board which was situated at 5 km distance from our test site. The mean RH, WS, SR and AT measured from 8 A.M. to 12 P.M. ranged from $26.86 \pm 3.31\%$ to $79.70 \pm 6.09\%$, 0.66 ± 0.16 m/s to 1.24 ± 0.35 m/s, 73.12 ± 6.57 W/m² to 483.52 ± 95.36 W/m², and 14.19 ± 2.53 °C to 34.10 ± 3.42 °C respectively as shown in the Table-7 and Fig. 8.

Table-7: Average weather conditions between 8 A.M. to 12 P.M. for 10 days of each month

Month	Av RH (%)	WS (m/s)	SR (W/m ²)	AT (°C)
Jun-20	46.47 ± 5.20	0.99 ± 0.32	483.52 ± 95.36	33.86 ± 2.94
Jul-20	55.47 ± 7.21	1.24 ± 0.35	379.59 ± 80.14	34.10 ± 3.42
Aug-20	58.26 ± 4.70	1.17 ± 0.51	361.35 ± 128.97	33.28 ± 1.36
Sep-20	58.92 ± 2.83	0.94 ± 0.35	297.20 ± 59.55	32.19 ± 0.80
Oct-20	46.84 ± 2.22	0.86 ± 0.18	171.02 ± 24.66	30.33 ± 1.19
Nov-20	49.34 ± 5.12	0.66 ± 0.16	99.91 ± 14.85	21.24 ± 0.82
Dec-20	61.86 ± 7.39	0.74 ± 0.17	73.12 ± 6.57	19.00 ± 1.46
Jan-21	79.70 ± 6.09	0.81 ± 0.21	75.44 ± 21.64	14.19 ± 2.53
Feb-21	65.13 ± 8.30	0.90 ± 0.24	111.38 ± 16.99	16.66 ± 2.46
Mar-21	46.34 ± 4.37	1.06 ± 0.30	96.02 ± 11.73	25.02 ± 2.45
Apr-21	26.86 ± 3.31	1.00 ± 0.26	232.53 ± 18.77	30.87 ± 1.92

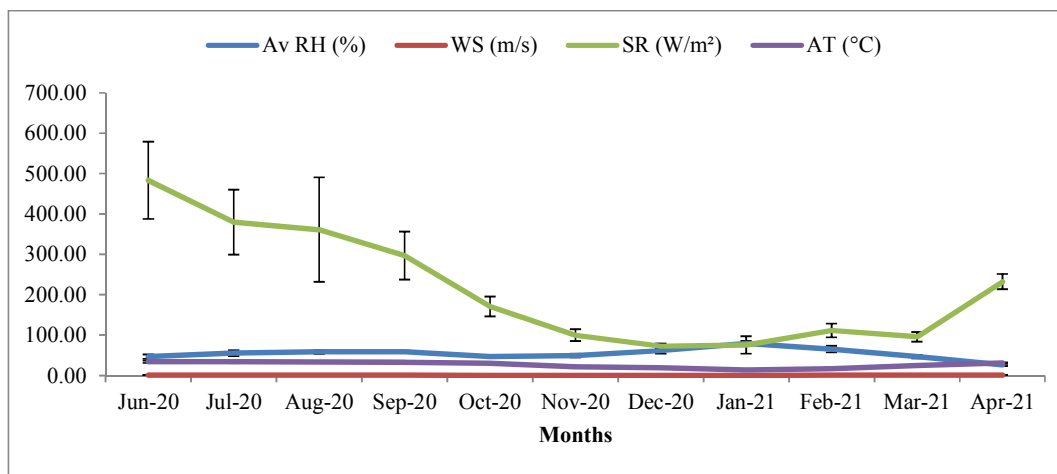


Fig. 8. Average weather conditions between 8 A.M. to 12 A.M. for 10 days of each month

During the 4 P.M. to 8 A.M. period the mean RH, WS, SR and AT varied from 23.85 ± 1.95 % to 23.85 ± 1.95 %, 0.32 ± 0.07 m/s to 1.15 ± 0.32 m/s, 15.01 ± 0.43

W/m^2 to 103.69 ± 35.96 W/m^2 and 15.73 ± 1.83 °C to 34.69 ± 3.24 °C respectively as depicted in Table-8 and Fig. 9.

Table-8: Average weather conditions between 4 P.M. to 8 P.M. for 10 days of each month with standard deviation

Month	Av RH (%)	WS (m/s)	SR (W/m ²)	AT (°C)
Jun-20	46.66 ± 7.60	1.02 ± 0.24	94.53 ± 37.93	33.46 ± 3.34
Jul-20	53.20 ± 7.24	1.15 ± 0.32	103.69 ± 35.96	34.69 ± 3.24
Aug-20	60.67 ± 6.24	1.12 ± 0.46	76.11 ± 26.70	32.73 ± 1.93
Sep-20	60.06 ± 5.54	1.04 ± 0.32	58.24 ± 21.01	31.53 ± 1.79
Oct-20	43.08 ± 1.46	0.78 ± 0.15	24.53 ± 5.15	31.09 ± 0.77
Nov-20	56.12 ± 6.91	0.32 ± 0.07	16.11 ± 0.72	21.10 ± 0.90
Dec-20	61.83 ± 4.63	0.37 ± 0.11	15.01 ± 0.43	19.86 ± 0.94
Jan-21	74.29 ± 12.0	0.87 ± 0.27	18.32 ± 3.94	15.73 ± 1.83
Feb-21	57.84 ± 5.16	0.81 ± 0.43	23.21 ± 1.09	19.43 ± 1.79
Mar-21	42.76 ± 3.42	0.89 ± 0.22	23.90 ± 4.50	27.19 ± 2.03
Apr-21	23.85 ± 1.95	0.93 ± 0.17	46.90 ± 6.42	33.06 ± 1.56

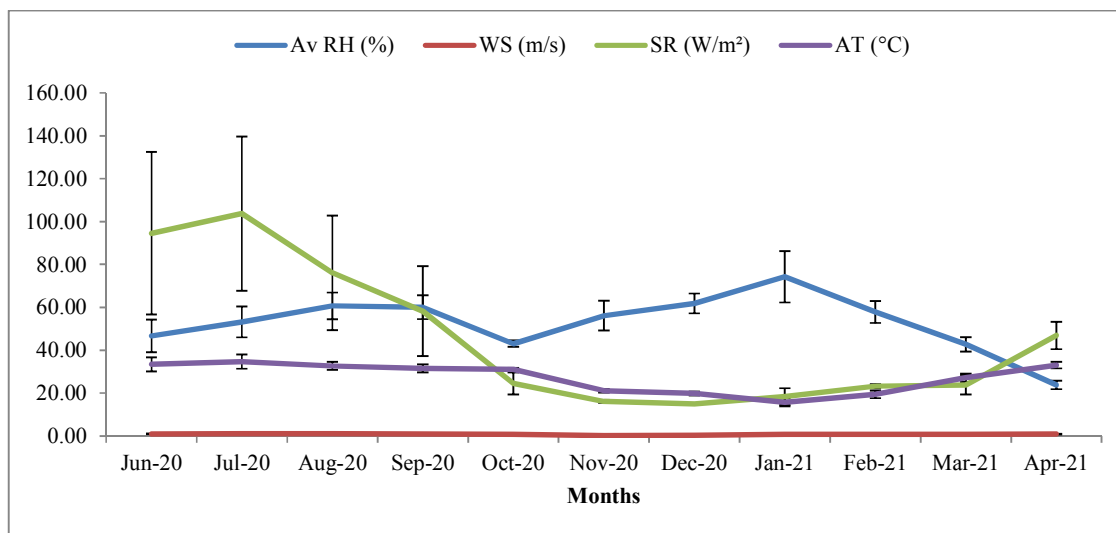


Fig. 9. Average weather conditions between 4 P.M. to 8 P.M. for 10 days of each month with standard deviation

During the 12 A.M. to 4 A.M. observational period the mean RH, WS, SR and AT varied from $32.89 \pm 3.37\%$ to $84.65 \pm 9.52\%$, 0.52 ± 0.14 m/s to $1.14 \pm$

0.41 m/s, 7.67 ± 0.92 W/m² to 10.68 ± 0.87 W/m² and 12.65 ± 3.0 °C to 330.22 ± 2.09 °C respectively as shown in Table-9 and Fig. 10.

Table-9: Average weather conditions between 12 A.M. to 4 A.M. for 10 days of each month with standard deviation

Month	Av RH (%)	WS (m/s)	SR (W/m ²)	AT (°C)
Jun-20	61.16 ± 5.48	0.60 ± 0.17	10.68 ± 0.87	27.69 ± 2.36
Jul-20	66.60 ± 6.80	1.14 ± 0.41	10.23 ± 0.89	30.22 ± 2.09
Aug-20	71.92 ± 5.22	0.91 ± 0.48	8.08 ± 1.55	29.12 ± 1.12
Sep-20	75.11 ± 4.56	0.65 ± 0.19	8.37 ± 1.06	27.36 ± 1.43
Oct-20	65.56 ± 2.91	0.59 ± 0.06	9.68 ± 0.66	23.37 ± 0.81
Nov-20	65.70 ± 8.98	0.54 ± 0.07	9.73 ± 0.83	15.39 ± 0.93
Dec-20	78.06 ± 6.19	0.52 ± 0.14	8.64 ± 0.94	13.95 ± 1.88
Jan-21	84.65 ± 9.52	0.60 ± 0.16	9.61 ± 1.11	12.65 ± 3.00
Feb-21	83.83 ± 5.89	0.55 ± 0.14	9.18 ± 0.99	12.40 ± 2.04
Mar-21	60.05 ± 6.63	0.69 ± 0.20	7.67 ± 0.92	19.53 ± 2.27
Apr-21	32.89 ± 3.37	0.92 ± 0.43	8.28 ± 1.14	23.94 ± 2.75

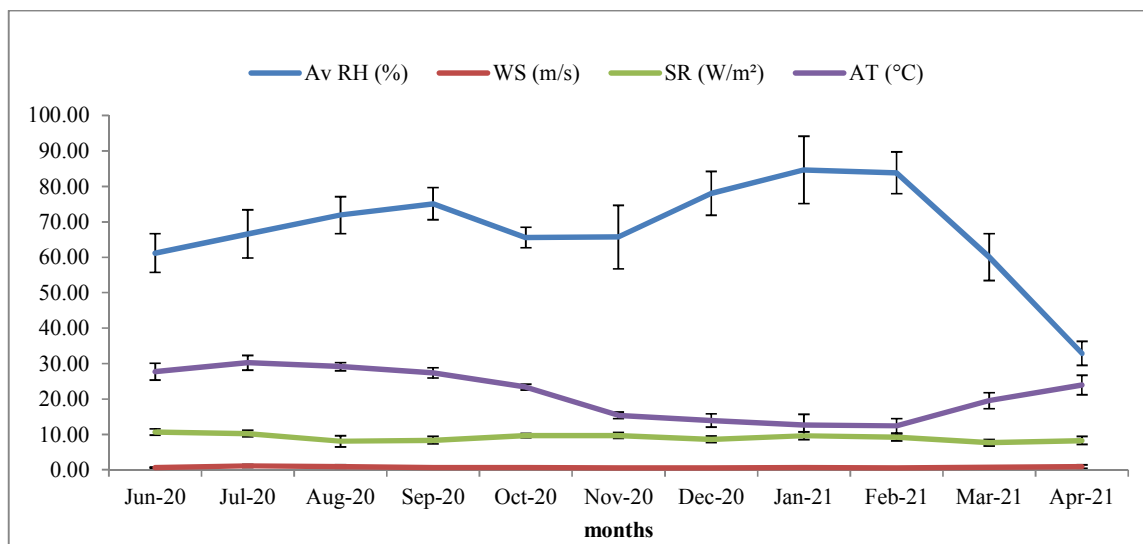


Fig. 10. Average weather conditions between 12 A.M. to 4 A.M. for 10 days of each month with standard deviation

5. DISCUSSION:

The increase in air pollution levels in the urbanized area of Delhi has become a major problem for a few years now and it poses a great health risk. Forecasting air pollution is not easy in large urban areas because the air pollutants emitted from numerous concentrated sources, as well as area sources, were dispersed over the entire geographical area [30]. In a study conducted by Singh & Kulshrestha [31] data on seasonal variation revealed that gaseous NH_3 concentrations peaked during the monsoon season. This could be because plants and other biological material decay and decompose under moist conditions, emitting NH_3 , which is why the monsoon season has the highest levels of NH_3 emissions. Additionally, seasonality in agricultural sources and manure application may have a greater impact on rural sites than the current urban location. In all seasons, it was observed that particulate NH_4^+ was consistently lower than ammonia gas. Due to higher humidity levels, the percent composition of particle NNH_4^+ was most observable during monsoon season. The amount of gaseous ammonia was found to be larger at night than during the day, due to greater atmospheric stability at night and a consequent reduction in the dispersion of this gas, which is normally released from low-level sources [31]. From 2011-2017, the ambient air quality deteriorated with increased pollutant concentration in the Delhi region at an

alarming rate [32]. Typically, Ammonia (NH_3) is present at higher concentrations in indoor air (~10-70 ppb) than in outdoor air (~50 ppt to 5 ppb). It acts as a dominant neutralizer of acidic species in indoor environments, strongly influencing the partitioning of gaseous acidic and basic species to aerosols, surface films, and bulk water [21].

One short-lived pollutant that significantly contributes to anthropogenic aerosols is nitrogen dioxide (NO_2) [33]. The volatilization of agricultural crops, animal waste, wastewater, and human excreta are just a few of the sources where anthropogenic activities are causing emissions of NO_x , N_2O , and NH_3 [34]. According to a research done in New York City, locations with high anthropogenic activity, such as traffic, building density, and built-up land uses, had the highest amounts of NO_2 [35] and the similar results were obtained in this study wherein the L1 showed the greater NO_2 load compared to L2 which has lower human activity, traffic building density and human settlement. In this study a positive correlation, 0.382 and 0.13, was found between the concentration of NH_3 and NO_2 in all the three observational periods at both the sites of testing. The formation of secondary particulate nitrate that contributes a major portion to the mass of particulate matter (P.M.) makes nitrogen dioxide (NO_2) play an important role. P.M. has several impacts on the environment on the scales of local, regional and global. NO_2 is regulated in most countries,

as it acts as a precursor for nitrate formation and shows significant negative effects on human health. There has been an increase in Nitrogen oxide (NO_x) emissions from the power sector by at least 70% from 1996 to 2010 because of rapid economic growth and consequent demand for electricity [36]. The estimated NO_x emissions from India were 9.3 Tg/yr in 2010, which is approximately 1/3 of those of China. This makes India the third largest emissions source after China (29.0 Tg/yr) and the US (13.4 Tg/yr) according to the Task Force Hemispheric Transport of Air Pollution version 2.2 inventories [37].

Tropospheric ozone (O₃) is a significant surface air pollutant, the main source of the hydroxyl radical, and the third most important greenhouse gas in the atmosphere. It is a key oxidant playing an essential role in atmospheric chemistry. Since 2000, emissions of O₃ precursors (NO_x and VOC's) in both China and India have increased dramatically due to the rapid growth of industrialisation, urbanisation, and transportation activities [38]. The upper troposphere O₃ is mainly produced by a catalytic reaction including NO_x. Emitted Nitrogen oxides react with forming NO₂. via photo-dissociation, NO₂ forms reactive ground state oxygen atom, O(³P) and it leads to the production of O₃ [39]. Experimental and epidemiological studies prove that short-term exposure to ozone has adverse health effects. The epidemiological evidence from individual-level panel studies has shown associations with changes in lung function in healthy subjects and symptom exacerbation and increased medication use in asthmatic subjects [40]. It has been seen that exposure to 18-20 hours of O₃ alters the epithelial permeability of the lung. The lung's mucociliary function is also acutely stimulated by O₃. Due to these effects, there is a possibility of an increase in susceptibility to bacterial respiratory infections. Exposure to ambient levels of O₃ for 6.6 hours has been shown to increase the markers of inflammation like the Neutrophils (PMNs), Prostaglandin E2 (PGE2), fibronectin, Interleukin-6 (IL-6), and Lactate Dehydrogenase (LDH), α-1 antitrypsin in the lungs, and decrease phagocytosis *via* the complement receptor. It has been seen that there can be a drop in lung function measures such as lung volume and expiratory flow rates, forced vital capacity and specific airway after

exposure to ambient-level O₃ concentrations [41]. Substantial but unique seasonal changes in O₃ have been reported in China and India, and they have been connected to greater precursor gas emissions and the summer monsoon season [42-45]. The present study at the two sites of open and covered drain showed that ozone in atmosphere increased in the afternoon and was monitored in higher concentration in the evening hours as compared to the midnight and morning hours. Ozone concentration varies with the solar radiation, traffic load and other anthropological activities that generate other pollutants like NO₂. It showed a positive correlation with solar radiation of 0.87 and 0.86 in the morning and evening monitoring at site L2 and 0.82 and 0.87 at the L1 site.

The biggest sources of SO₂ emissions are burning of fossil fuels in power plants and industries SO₂ is a highly reactive gas. Furthermore serving as a cooling agent, SO₂ is a major precursor of anthropogenic aerosols in the atmosphere. According to some earlier research, even a brief exposure to high SO₂ levels can have a negative impact on breathing. Short-term exposure to daily SO₂ was linked with an elevated risk of asthma in terms of asthma-associated expiratory reserve volumes [46]. The present study revealed that the concentration of SO₂ has come down substantially due to the improvement of fuels used in vehicles as well as the increase in the number of CNG vehicles on the road. However the variation pattern similar to other pollutants was followed by SO₂ as well. Maximum pollution was observed in the month of October and November 2020 which gradually decreased in the winter months of December 2020 and January and February 2021. The two months of summer March and April 2021 showed an upward trend in pollution due to all the four gases studied. Diurnal variation was also observed in all the four criteria pollutants studied. Maximum pollution load was observed in the evening 4 P.M. to 8 P.M. hours and the least was observed after the midnight (12 A.M. to 4 A.M.) at both sites L1 and L2.

Conclusion

The study showed that the concentration of all chemical air parameters are dependent on the

population density, traffic density, open space for dispersal and local environmental condition of the area. The concentration of NO₂, SO₂, NH₃ and O₃ was found more at location with covered drain near the vents 100% times in the morning 8 A.M. to 12 P.M. duration. In the 4 P.M. to 8 P.M. duration NO₂, SO₂ and O₃ were more for 100% times at covered drain however NH₃ was more for 90.9 % times. The after midnight period of monitoring showed O₃ to be 100% times greater covered drain site but NO₂, SO₂ and NH₃ were 81.8%, 72.2% and 90.9% times more at covered drain with road built over it. The highest total average pollution due to NO₂, SO₂, NH₃ and O₃ was $37.4 \pm 6.37 \mu\text{g}/\text{m}^3$, $16.53 \pm 2.78 \mu\text{g}/\text{m}^3$, $41.58 \pm 7.50 \mu\text{g}/\text{m}^3$ and $37.82 \pm 9.56 \mu\text{g}/\text{m}^3$ respectively in the evening monitoring period of 4 P.M. to 8 P.M. at the covered drain site. This can be attributed to higher vehicular flow during these hours. Least concentration of all pollutants was found after midnight hours. However the overall pollution load was found to be more around the covered drain with road over it throughout the year than the open drain area having green catchment area due to more vehicular traffic, population density and less space for pollutant dispersal.

REFERENCES:

1. E.I. Clinton, A. Agbakoba and P.W. Igbagara, *TLEP Int. J. Appl. Chem. Ind. Sci.*, **2**, 11 (2016).
2. D.E. Schraufnagel, J.R. Balmes, C.T. Cowl, S. De Matteis, S.-H. Jung, K. Mortimer, R. Perez-Padilla, M.B. Rice, H. Riojas-Rodriguez, A. Sood, G.D. Thurston, T. To, A. Vanker and D.J. Wuebbles, *Chest*, **155**, 417 (2019).
3. B.R. Gurjar, K. Ravindra and A.S. Nagpure, *Atmos. Environ.*, **142**, 475 (2016).
4. 2020 World Air Quality Report (Region & City PM2.5 Ranking), IQAir's online air quality information platform (2020).
5. P.S. Monks, A.T. Archibald, A. Colette, O. Cooper, M. Coyle, R. Derwent, D. Fowler, C. Granier, K.S. Law, G.E. Mills, D.S. Stevenson, O. Tarasova, V. Thouret, E. von Schneidemesser, R. Sommariva, O. Wild and M. L. Williams, *Atmos. Chem. Phys.*, **15**, 8889 (2015).
6. X. Lu, L. Zhang, X. Liu, M. Gao, Y. Zhao and J. Shao, *Atmos. Chem. Phys.*, **18**, 3101 (2018).
7. C.S. Malley, D.K. Henze, J.C. Kuylenstierna, H.W. Vallack, Y. Davila, S.C. Anenberg, M.C. Turner and M.R. Ashmore, *Environ. Health Persp.*, **125**, 087021 (2017).
8. P. Yin, R. Chen, L. Wang, X. Meng, C. Liu, Y. Niu, Z. Lin, Y. Liu, J. Liu, J. Qi, J. You, M. Zhou and H. Kan, *Environ. Health Persp.*, **125**, 117006 (2017).
9. Y. Chen, O. Wild, E. Ryan, S.K. Sahu, D. Lowe, S. Archer-Nicholls and G. Beig, *Atmos. Chem. Phys.*, **20**, 499 (2020).
10. S.A. Meo, A.A. Abukhalaf, W. Sami and T.D. Hoang, *J. King Saud Univ. Science*, **33**, 101373 (2021).
11. A. Siddiqui, S. Halder, P. Chauhan and P. Kumar, *J. Indian Soc. Remote Sens.*, **48**, 999 (2020).
12. A.K. Pandey, R.P. Kumar and K. Kumar, Satellite and Ground-Based Seasonal Variability of NO₂ and SO₂ over New Delhi, India. In Remote Sensing of Clouds and the Atmosphere XX, SPIE, vol. 9640, pp. 212-218 (2015).
13. S. Bootdee, P. Chalemrom and S. Chantara, *Int. J. Environ. Sci. Technol.*, **9**, 515 (2012).
14. M.J. Bechle, D.B. Millet and J.D. Marshall, *Atmos. Environ.*, **69**, 345 (2013).
15. O.K. Kurt, J. Zhang and K.E. Pinkerton, *Curr. Opin. Pulm. Med.*, **22**, 138 (2016).
16. S.S. Braman, *Chest*, **129**, 104S (2006).
17. X. Huang, R. Qiu, C.K. Chan and P.R. Kant, *Atmos. Res.*, **99**, 488 (2011).
18. V. Masson-Delmotte et al., Eds. Intergovernmental Panel on Climate Change (IPCC), Summary for Policymakers in Climate Change 2021: The Physical Science Basis. Contribution of Working Group I to the Sixth Assessment Report of the Intergovernmental Panel on Climate Change, Cambridge Univ. Press (2021).
19. Y. Nagata, *Odor. Meas. Rev.*, **118**, 118 (2003).
20. S.N. Behera, R. Betha and R. Balasubramanian, *Aerosol Air Qual. Res.*, **13**, 1282 (2013).

21. M. Li, C.J. Weschler, G. Beko, P. Wargoeki, G. Lucic and J. Williams, *Environ. Sci. Technol.*, **54**, 5419 (2020).
22. R.P. Padappayil and J. Borger, Ammonia Toxicity, In: StatPearls Treasure Island (FL): StatPearls (2022).
23. WHO, Ambient (outdoor) Air Pollution; [https://www.who.int/news-room/fact-sheets/detail/ambient-\(outdoor\)-air-quality-and-health](https://www.who.int/news-room/fact-sheets/detail/ambient-(outdoor)-air-quality-and-health) (2019).
24. National Ambient Air Quality Status (NAAQS), Central Pollution Control Board Ministry of Environment & Forests, Government of India (2009).
25. World Health Organization. Air Quality Guidelines - Update 2021. Copenhagen, Denmark: WHO Regional Office for Europe (2021).
26. I. Abd-Elaty, A. Kuriqi & A. El Shahawy, *Nat. Hazards*, **110**, 2353 (2022).
27. IS 5182 (Part 6): Methods for Measurement of Air Pollution and the Meteorological Parameters, Temperature, Wind Speed and Relative Humidity, In: Guidelines for the Measurement of Ambient Air Pollutants (2013).
28. IS 5182 (Part 9): CPCB (2009). National Ambient Air Quality Standards (NAAQS).
29. IS 5182 (Part 25): CPCB, Guidelines for the Measurement of Ambient Air Pollutants (2013).
30. D. Mishra and P. Goyal, *Aerosol Air Qual. Res.*, **16**, 166 (2016).
31. S. Singh and U.C. Kulshrestha, *Biogeosciences*, **9**, 5023 (2012).
32. N. Sharma, S. Taneja, V. Sagar and A. Bhatt, *Procedia Comput. Sci.*, **132**, 1077 (2018).
33. J.H. Seinfeld and S.N. Pandis, Atmospheric Chemistry and Physics: From Air Pollution to Climate Change, Wiley, Edn. 3 (2016).
34. V.P. Aneja, W.H. Schlesinger, J.W. Erisman, S.N. Behra and M. Sharma, *Atmos. Environ.*, **47**, 92 (2012).
35. New York City Department of Health and Mental Hygiene (2020).
36. Z. Lu and D.G. Streets, *Environ. Sci. Technol.*, **46**, 7463 (2012).
37. G. Janssens-Maenhout, M. Crippa, D. Guizzardi, F. Dentener, M. Muntean, G. Pouliot, T. Keating, Q. Zhang, J. Kurokawa, R. Wankmüller, H. Denier van der Gon, J.J.P. Kuenen, Z. Klimont, G. Frost, S. Darras, B. Koffi and M. Li, *Atmos. Chem. Phys.*, **15**, 11411 (2015).
38. A. Hilboll, A. Richter and J. P. Burrows, *Atmos. Chem. Phys.*, **13**, 4145 (2013).
39. S. Rosanka, C. Frömming and V. Grewe, *Atmos. Chem. Phys.*, **20**, 12347 (2020).
40. R.W. Atkinson, D. Yu, B.G. Armstrong, S. Pattenden, P. Wilkinson, R.M. Doherty, M.R. Heal and H.R. Anderson, *Environ. Health Persp.*, **120**, 1411 (2012).
41. B. Sujith and M. Sehgal, *Int. J. Med. Public Health*, **7**, 56 (2017).
42. S. Lal, M. Naja and B.H. Subbaraya, *Atmos. Environ.*, **34**, 2713 (2000).
43. S.D. Ghude, C. Jena, D.M. Chate, G. Beig, G.G. Pfister, R. Kumar and V. Ramanathan, *Geophys. Res. Lett.*, **41**, 5685 (2016).
44. X. Lu, J. Hong, L. Zhang, O.R. Cooper, M.G. Schultz, X. Xu, T. Wang, M. Gao, Y. Zhao and Y. Zhang, *Environ. Sci. Technol.*, **5**, 487 (2018).
45. T. Wang, L. Xue, P. Brimblecombe, Y.F. Lam, L. Li and L. Zhang, *Sci. Total Environ.*, **575**, 1582 (2017).
46. X.-Y. Zheng, P. Orellano, H.-L. Lin, M. Jiang and W.-J. Guan, *Environ. Int.*, **150**, 106435 (2021).